

Photoionization of Three Isomers of the C₉H₇ Radical[†]Patrick Hemberger,[‡] Michael Steinbauer,[‡] Michael Schneider,[‡] Ingo Fischer,^{*,‡} Melanie Johnson,[§] Andras Bodi,[§] and Thomas Gerber^{*,§}

Institute of Physical Chemistry, University of Würzburg, Am Hubland, D-97074 Würzburg, Germany, and Paul Scherrer Institut, Villigen 5232, Switzerland

Received: July 20, 2009; Revised Manuscript Received: August 24, 2009

Three resonance-stabilized radicals, 1-indenyl (Ind), 1-phenylpropargyl (1PPR), and 3-phenylpropargyl (3PPR), all isomers of the composition C₉H₇, were generated by jet flash pyrolysis. Their photoionization was examined by VUV synchrotron radiation. The mass spectra show a clean and efficient radical generation when the pyrolysis is turned on. To study the photoionization, photoion yield measurements and threshold photoionization spectroscopy techniques were applied. We determined adiabatic ionization energies (IE_{ad}) of 7.53 eV for Ind, 7.20 eV for 3PPR, and 7.4 eV for 1PPR. Ab initio calculations show no major change in geometry upon ionization, in agreement with ionization from a nonbonding molecular orbital. The IEs were also computed and are in agreement with the measured ones. The difference in the IE might allow a distinction of the three isomers in flames. In the indenyl spectrum, an excited a⁺ ³B₂ state of the cation was identified at 8.10 eV, which shows a low-energy vibrational progression of 61 meV. Furthermore, we have examined the dissociative photoionization of the precursors. The indenyl precursor, 1-indenyl bromide, undergoes dissociative photoionization to Ind⁺. An appearance energy (AE_{OK}) of 10.2 eV was obtained from fitting the experimental breakdown diagram. A binding energy of 1.8 eV can thus be determined for the C–Br bond in 1-indenyl bromide. The phenylpropargyl precursors 1PPBr (1-phenylpropargyl bromide/3-phenyl-3-bromopropyne) and 3PPBr (3-phenylpropargyl bromide/1-phenyl-3-bromopropyne) also lose a bromine atom upon dissociative photoionization. Approximate appearance energies of 9.8 eV for 3PPBr and 9.3 eV for 1PPBr have been determined.

Introduction

In this paper, we present photoionization yield, threshold photoelectron, and threshold photoelectron photoion coincidence (TPEPICO) spectra of the 1-indenyl (Ind), 3-phenylpropargyl (3PPR), and 1-phenylpropargyl radicals (1PPR), produced by vacuum jet flash pyrolysis¹ (Figure 1), applying synchrotron radiation in the vacuum ultraviolet (VUV) energy range. As visible in Figure 1, the corresponding bromides were used as precursors. The precursor for 1-PPR is 3-phenyl-3-bromopropyne (center trace), and the one for 3PPR is termed 1-phenyl-3-bromopropyne (bottom trace). To make the relationship between radical and precursor unambiguous, we will use from hereon the shorthand notations IndBr (indenyl bromide), 1PPBr (1-phenylpropargyl bromide), and 3PPBr (3-phenylpropargyl bromide) for the precursor molecules. All of the radicals have the same composition, C₉H₇, and are precursors in soot formation. In previous experiments, we have shown the potential of synchrotron radiation studies in connection with coincidence spectroscopy for determining ionization or appearance energies of reactive intermediates. For example, the thresholds for the dissociative photoionization of allyl, ethyl, and propargyl were identified,^{2–4} and recently, the ionization energies of two phenylcarbenes and the dissociative photoionization of their precursors were measured.⁵

Radicals play an important role in the formation of polycyclic aromatic hydrocarbons (PAH) and soot in flames. Photoioniza-

tion utilizing synchrotron radiation can be employed to monitor their concentrations in flames online, as has been shown in the literature.^{6–9} However, ionization and appearance energies of radicals and their precursors have to be known beforehand to distinguish between structural isomers in flames.

Only few spectroscopic data are available in the literature for the three reactive intermediates examined in this paper. The ionization energy of Ind was first measured by Pottie and Lossing.¹⁰ They report an adiabatic ionization energy (IE_{ad}) of 8.35 eV by electron impact techniques. Furthermore, Izumida et al. published an emission and excitation spectrum of indenyl in a 3-methylhexane matrix at 7 K.¹¹

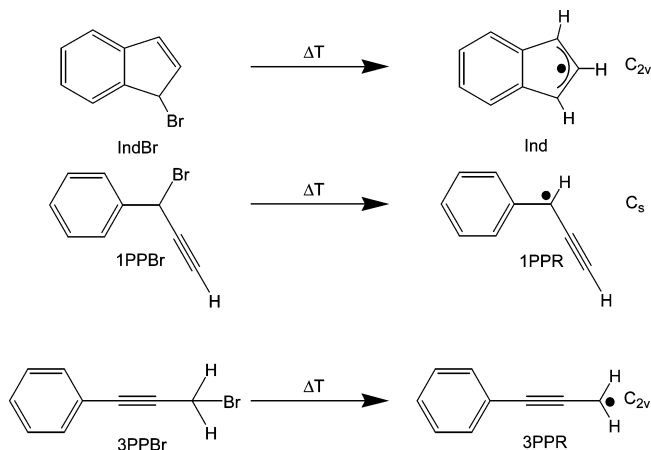


Figure 1. The three C₉H₇ isomers were produced by vacuum jet flash pyrolysis from their bromine precursors. Also, the point group of each radical is given on the right-hand side.

[†] Part of the special section “30th Free Radical Symposium”.

^{*} To whom correspondence should be addressed. E-mail: ingo@phys-chemie.uni-wuerzburg.de (I.F.); Thomas.Gerber@psi.ch (T.G.).

[‡] University of Würzburg.

[§] Paul Scherrer Institut.

Only approximate experimental ionization energies are available for either of the phenylpropargyl radicals. Andrews and Kelsall first observed 3PPR in a discharge experiment with phenylacetylene in a 20 K argon matrix and identified it by its UV spectrum.¹² The laser-induced fluorescence (LIF) and single vibronic level fluorescence spectrum (SVLF) of 1PPR were reported by Reilly et al.^{13,14} They synthesized 1PPR in an electrical discharge source with benzene as a precursor and identified it by multiphoton ionization (MPI) and LIF spectroscopy. Apart from C₂, C₃, and CH, 1PPR was the most brightly fluorescing substance in the LIF spectrum. According to the authors, the ring breathing, the ring deformation, and the C–C stretching vibrations in the side chain have the highest Franck–Condon factors, and the transition is of mixed $\pi n/n\pi^*$ character. Both the ground (D₀) and excited states (D₁) are of A'' symmetry. With these techniques, the authors could assign almost half of the 42 frequencies in each state. From the MPI experiments, they concluded that the IE has to be between 5.1 and 7.3 eV.

The most likely step in the formation of PAHs is the dimerization of two propargyl radicals with a hydrogen abstraction forming an aromatic C₆H_n ring.^{15–17} Further addition of C₃H₃ and H-abstraction creates a phenylpropargyl radical, which, according to Stein et al.,¹⁸ can be involved in a number of further reactions, two examples of which are the generation of *o*-terphenyl in a dimerization process and the formation of a doubly substituted 1,5-hexadiyne.

It is the aim of this study to determine IEs of the three C₉H₇ isomers, which may permit an isomer-selective detection of these radicals in flames.

Experimental Section

The experiments were carried out at the VUV beamline of the Swiss Light Source at the Paul Scherrer Institut (PSI) in Villigen, Switzerland. Only a brief overview is given here because the setup of the beamline is described in detail elsewhere.^{19,20} The X04DB bending magnet provides synchrotron radiation, which is collimated by a platinum-coated copper mirror and sent to a plane grating monochromator. The 600 grooves·mm⁻¹ grating is optimized for the 5–15 eV energy range and has a resolving power of 10⁴. The beam is focused by another mirror onto the 110–1000 μ m vertical exit slits of the monochromator, which are located inside of a rare gas filter. This filter operates at a pressure of 10–13 mbar to suppress the higher harmonic radiation. For photon energies below 8 eV, either a MgF₂ window or a gas mixture (Ne, Ar, Xe) is used, and between 8 and 10.5 eV, an Ar–Ne mixture is used. The flux is approximately 10¹¹ photons/s in the energy range between 6.5 and 10.5 eV employed in the present study.²⁰ A photon energy resolution of 5 meV was achieved at 15.764 eV, measured at the 11s' peak of argon with fully open horizontal slits.

Experiments were performed in a differentially pumped vacuum chamber employing a supersonic molecular beam apparatus. The (T)PEPICO technique was used to study the photoionization of the radicals and the dissociative photoionization of the precursors.^{21,22} The spectrometer combines a velocity map imaging electron spectrometer²³ and a Wiley–McLaren TOF mass spectrometer.¹⁹ Electrons are accelerated with a constant field of 40 or 80 V/cm and focused by a potential of 144 or 273 V onto the microchannel plates (MCPs) of a position-sensitive detector with a delay line anode (Roentdek DLD40). Threshold electrons were typically selected with an energy resolution of 5 meV. The contribution of hot background

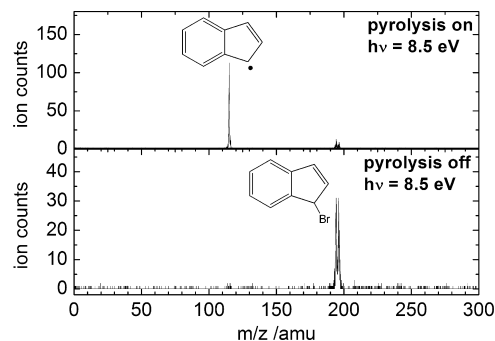


Figure 2. Photoionization mass spectra of IndBr (lower trace) and Ind ($m/z = 115$) with active pyrolysis (upper trace) at 8.5 eV.

electrons was subtracted following the method outlined by Baer and co-workers.^{24,25} Ions are extracted by a field of 40 or 80 V/cm and further accelerated to -550 V within a distance of 10 mm. At the end of a 550 mm long-field free drift tube, the ions are detected by MCPs.

On the vacuum chamber, we mounted a flange with a continuous molecular beam source coupled with a pyrolysis tube.¹ A heated silicon carbide (SiC) tube was mounted onto the faceplate (orifice 100 or 150 μ m) of a General Valve, operating without a poppet and augmented by a water cooling system. In order to avoid bimolecular reactions, the heating electrodes were fixed together as close as possible at the end of the tube. Due to the continuous gas flow and the small orifice, the beam temperature was higher than that in the case of a pulsed molecular beam, and cooling of the internal degrees of freedom was less efficient.

We used 3PPBr and 1PPBr as precursors for the PPR and IndBr for the generation of indenyl radicals. All precursors were synthesized as published in the literature.^{26–28} The compounds were seeded in either 0.25 or 0.6 bar (absolute) of argon and expanded through the SiC tube. We adjusted the heating power in order to get full conversion of the precursors (strong orange glowing of the SiC tube). Most of the spectra were averaged for 120 s per data point and normalized to the photon flux, which was measured previously by a photodiode.²⁰

Results and Discussion

a. Indenyl Radical. In a first step, we recorded mass spectra in order to ensure that the reactive intermediates were formed cleanly. Figure 2 shows mass spectra of IndBr at 8.5 eV photon energy with pyrolysis on (upper trace) and off (lower trace). In the lower trace, the precursor (IndBr) with its bromine isotopic pattern at $m/z = 194$ and 196 is visible. Note that no dissociative photoionization of the precursor was observed at this energy. When the pyrolysis was turned on, the precursor signal almost disappeared, and a strong signal at $m/z = 115$ (upper trace) was detected, which was assigned to the Ind. We found no evidence of dimerization of the radical or other side products coming from the pyrolysis, as has been reported in earlier experiments using synchrotron radiation.³ Only a small precursor signal remained; therefore, almost full conversion into the radical was achieved. Small traces of indene from the synthesis were also visible.

Before studying the photoionization of the reactive intermediate, the photoionization and dissociative photoionization of the precursor have to be analyzed because it can generate fragment ions that are mistakenly assigned to the cation of the radical. Therefore, we measured the signal intensity of the precursor as a function of the photon energy while the pyrolysis was turned

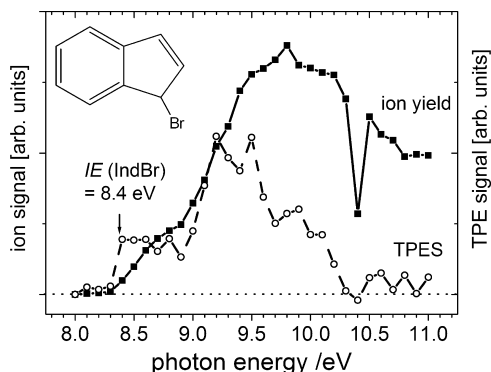


Figure 3. Photoion yield and TPES of IndBr. The signal sets in at 8.4 eV, which constitutes an approximate IE_{ad} .

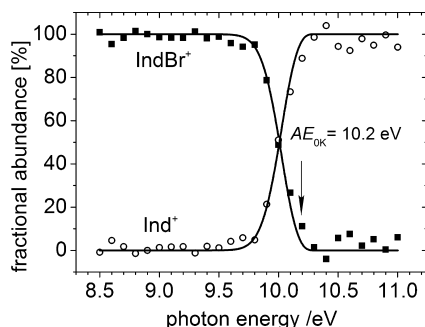


Figure 4. Breakdown diagram of $IndBr^+/Ind^+$. A fit to the experimental data (solid line) yields $AE_{0K} = 10.2$ eV

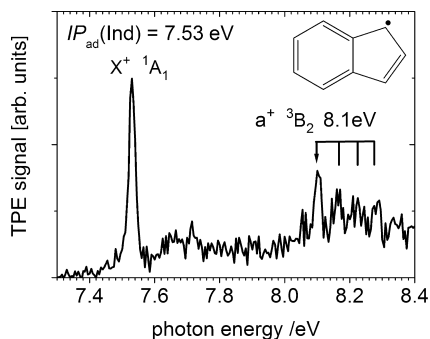
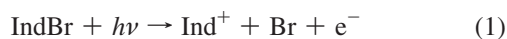


Figure 5. TPES of the 1-indenyl radical. We assigned the first band to $IE_{ad} = 7.53$ eV. The first excited electronic state of the cation appears at 8.10 eV and shows a low-energy progression of around 61 meV.

off. In Figure 3, such a spectrum is depicted. The photon energy was scanned with a step size of 0.1 eV. The ion signal of IndBr increased at about 8.4 eV. The ionization energy can be derived more accurately if we look only at the ion signal in coincidence with threshold photoelectrons (TPE). The dashed line in Figure 3 shows this mass-selected TPE signal as a function of photon energy. One can extract a value of 8.4 eV for the adiabatic ionization energy of indenyl bromide.

The analysis of the dissociative photoionization of IndBr is based on the breakdown diagram depicted in Figure 4. It shows the fractional abundance of the parent and the daughter ion (Ind^+). Note that we used the threshold electron signals of $IndBr^+$ and Ind^+ in this diagram. The dissociation proceeds according to eq 1.



As visible in Figure 4, energy-selected IndBr ions show fragmentation in the energy range between 9.7 and 10.2 eV,

and the crossover point between the parent and daughter signal lies at about 10 eV. The breakdown diagram is modeled by eqs 2–4 to extract the appearance energy at 0 K, AE_{0K} . $S_{parent}(h\nu)$ and $S_{daughter}(h\nu)$ denote the signals of the precursor and the fragment, which means that AE_{0K} is reflected by the disappearance of the parent ion in the breakdown diagram.^{24,29–31}

$$S_{parent}(h\nu) = \int_0^{AE-h\nu} P(E)dE \quad \text{for } h\nu < AE \quad (2)$$

$$S_{daughter}(h\nu) = \int_{AE-h\nu}^{\infty} P(E)dE \quad \text{for } h\nu < AE \quad (3)$$

$$S_{parent}(h\nu) = 0 \quad S_{daughter}(h\nu) = 1 \quad \text{for } h\nu > AE \quad (4)$$

$P(E)$ is the normalized thermal energy distribution of the parent molecule, which is given by $P(E) \sim \rho(E) \exp(-E/kT)$. The density of vibrational states $\rho(E)$ was calculated according to the Beyer–Swinehart algorithm.³² The frequencies of the precursor were calculated by DFT methods described below. From a least-squares fit of eqs 2–4, $AE_{0K} = 10.2$ eV is obtained.^{33,34} The best fit was achieved for a temperature of 300 K. This procedure assumes that all parent ions that have enough energy to dissociate will do so, that is, the dissociation is fast, and there is no kinetic shift. Parent ions that dissociate slowly ($10^3 < k < 10^7$ s⁻¹) in the acceleration region of the TOF analyzer contribute to asymmetric daughter ion peak shapes. At low energies, the Ind^+ is slightly asymmetric, but due to the large step size and the small signal levels, the presumably small kinetic shift was not included in the modeling.

Because of the large photon energy step size, the accuracy is probably limited to 0.1 eV, worse than both electron and photon resolution. With the appearance energy of the fragment and the ionization energy of the precursor known, the C–Br binding energy of the precursor cation $IndBr^+$ can be calculated, assuming that there is no reverse barrier along the reaction coordinates. Taking an $IE(IndBr)$ of 8.4 eV and $AE(IndBr, Ind^+) = 10.2$ eV, one arrives at 1.8 eV as the bond energy of C–Br in $IndBr^+$.

Once the necessary data of the precursor photoionization and dissociative photoionization are known, the photoionization of indenyl can be investigated. The pyrolysis is turned on, and the radical is produced by thermal cleavage of the C–Br bond. In Figure 5, the TPE signal of Ind^+ is plotted as a function of photon energy. Data were recorded with a 5 meV step size. The signal increased strongly at about 7.5 eV. At 7.7 eV, an additional broad band appeared, and at around 8.1 eV, a second band appeared.

We assign the first peak in the TPES to the ionization threshold. We took the maximum of the peak to obtain the adiabatic ionization energy (IE_{ad}). Hence, the measured IE_{ad} is 7.53 eV, with an estimated error of 20 meV. The full width at half-maximum (fwhm) of the peak of 23 meV is rather broad compared to the one observed for Ar, which showed a fwhm of only 5 meV. Thus, the broadening is not due to the bandwidth of the synchrotron radiation or the electron spectrometer. We regard this as an effect coming from insufficient cooling of the radical in the molecular beam. The small signal below 7.5 eV is assigned to hot bands, but sequence bands and the rotational envelope will contribute to the TPE signal as well. Because the spectrum is dominated by one intense peak, the geometry does not change strongly upon ionization, and Franck–Condon factors favor the transition from the vibrational ground state of

TABLE 1: Comparison of the Calculated IEs with the Experimental and Earlier Literature Values for Indenyl, 1-Phenylpropargyl, and 3-Phenylpropargyl

	IE _{exp} /eV	IE _{ad, calc} /eV	IE _{vert, calc} /eV	IE _{Lit} /eV
Ind	7.53	7.50	7.54	8.35 ¹⁰
3PPR	7.20	7.13	7.21	6.8 ¹³
1PPR	7.4	7.14	7.19	6.8 (comp)/ 5.1–7.3 eV (exp) ¹³

the neutral to the vibrational ground state of the cation. Another rather broad band appears with lower intensity at around 7.7 eV. It possibly originates from excited vibrational states of the cation. The third band around 8.10 eV is too high in energy for a vibrationally excited state. We exclude any contribution from indene (C₉H₈) to these peaks, which is present in small concentrations as a side product from the synthesis of IndBr and has an IE of 8.14 eV.³⁵ As supported by calculations (see below), the band corresponds most likely to the electronically excited a⁺ ³B₂ state of the indenyl cation, where the electron is removed from the HOMO-1 orbital. Closer inspection reveals further peaks separated by 61 meV, as indicated in Figure 5. They are assigned to a low-energy vibrational progression in the a⁺ ³B₂ state. Computations (see below) yielded a ring-deformation mode at 478 cm⁻¹, which is thus a possible carrier of the progression. When the ionization of the indenyl radical was first studied by electron impact ionization, the IE was determined to be 8.35 eV.¹⁰ Probably, the first excited state of the cation was found in this earlier work and not the ionic ground state. We also attempted to find the low-lying thresholds for dissociative photoionization of indenyl and recorded mass spectra at selected energies up to 15 eV. However, no fragments appeared that could be unambiguously assigned to this process.

In order to support the analysis of our experiments, we performed density functional theory (DFT) calculations. We used the Gaussian03 program package with the B3LYP exchange-correlation functional and the 6-311⁺⁺G** basis set.^{36,37} For the geometry optimization, a modified GDIIS algorithm (geometry optimization using direct inversion in the iterative subspace) was employed, and tight convergence criteria with an ultrafine grid were used.³⁸ The ground-state geometries of the radical and cation (singlet and triplet) were calculated, and the difference between the zero-point energies was taken as the IE_{ad}. As a guess for the vertical ionization energy, the energy of the cation was computed at the equilibrium geometry of the neutral ground state. To calculate the higher excited states of the cation at the ground-state geometry, we applied time-dependent DFT (TD-DFT) with a B3P86 functional and 6-311⁺⁺G** basis set.^{39,40}

Table 1 summarizes the results of our calculations and compares them to the experimental ionization energies and earlier literature values. A summary of bond lengths and angles is given in the Supporting Information. C_{2v} symmetry was found for both the radical and the cation in the calculations. The calculated ionization energies are in good agreement with the experiment and also give a substantially smaller value than the earlier experimental number.¹⁰ Also in agreement with the experiment, the computations suggest no major geometry change upon ionization of the 1-indenyl radical. Correspondingly, the difference between the IE_{ad} and IE_{vert} (7.50 and 7.54 eV) is small. The highest occupied molecular orbital (HOMO) of a₂ symmetry is distributed over the whole molecule. The nonbonding character of this HOMO explains the low change in geometry during ionization. We also found three vibrations of the cation in the energy range at around 1200 cm⁻¹ (0.149 eV) which might

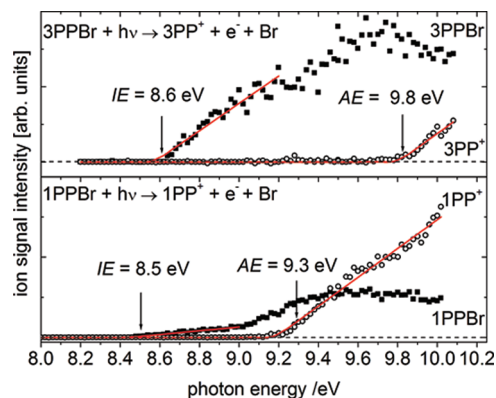


Figure 6. Photoionization and dissociative photoionization of the 1- and 3PPBr. The ion signal as a function of the photon energy is given in the graphs. Both precursors yield $m/z = 115$ as the product according to the reaction indicated in the graph. A fitting procedure yields the onset of fragmentation and the ionization energies.^{41,42}

be responsible for the band at around 7.7 eV. They correspond to C–H bending vibrations and to a ring breathing vibration. At least for the latter one, some activity is expected. Computations of the cationic excited singlet and triplet states yield a low-lying ³B₂ state at 7.94 eV (adiabatic ionization energy). This supports the assignment of the band at 0.6 eV above the ionization threshold to this excited triplet state. With respect to the radical, the electron is removed from the HOMO-1 orbital, which has b₁ symmetry. To summarize the results of the calculations, a comparison with the experimental data indicates that the method and basis set employed are adequate for the calculation of ionization energies of C₉H₇ isomers.

b. Phenylpropargyl Radicals. Phenylpropargyl radicals were generated in a similar way as indenyl. We used 1PPBr and 3PPBr as precursors for both intermediates. A clean and almost complete conversion of the precursor could be confirmed. The mass spectra of both species exhibit similar features to those of the indenyl radical. The precursors also show an isotopic pattern at $m/z = 194/196$ and disappear when the pyrolysis is turned on, while a signal at $m/z = 115$ arises that can be assigned to 1PPR or 3PPR. To exclude that the phenylpropargyl cations are formed by dissociative photoionization of the precursors, the photoionization and fragmentation of these molecules were examined as well. Figure 6 depicts the photoion yield of 3PPBr and 1PPBr and their dissociative photoionization products (3PP⁺ and 1PP⁺). The reaction equation for the dissociation is also given in the figure. All ions were recorded, not only those associated with threshold electrons, in contrast to the earlier experiments on indenyl bromide (cf. Figure 4); therefore, no breakdown diagram is available.

The upper part of Figure 6 shows the ion signal intensities of the 3PPBr parent and the 3PP⁺ daughter as a function of the photon energy. Ionization of the precursor sets in at about 8.6 eV, while the daughter mass (3PP⁺) appears above 9.8 eV. The ionization energy and onset of fragmentation were determined by a simple fitting procedure, convoluting a thermal energy distribution with a linear function, as suggested in the literature.^{41,42} The best fits were found for a temperature of 150 K. In a similar way, values for the onset of ionization and dissociative ionization can be obtained for 1PPBr and 1PP⁺. Here, the precursor ionizes at around 8.5 eV and starts dissociating above 9.2 eV. An approximate appearance energy of 9.3 eV is obtained from the fit. Coincidence data based on the detection of threshold electrons would yield more accurate data, as in the case of IndBr. However, the signal-to-noise ratio in the experiments on PPBr

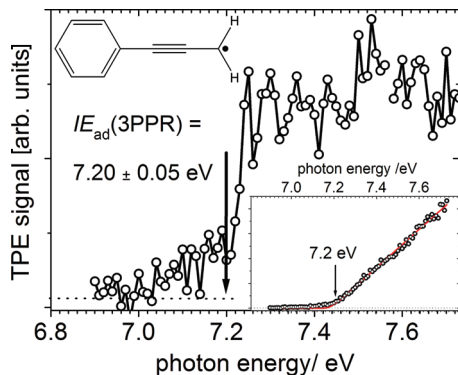


Figure 7. Threshold photoelectron spectrum of 3PPR showing a signal increase at 7.20 eV, assigned to the ionization threshold. The ion yield spectrum is shown in the inset. A fit of the photoion signal yielded the same value of 7.2 eV.

was too low, and a breakdown diagram of sufficient quality could not be recorded. Therefore, exact values for binding energies can also not be derived. Estimated binding energies of the C–Br bond in 3PPBr⁺ and 1PPBr⁺ are 1.2 and 0.7 eV, respectively, significantly lower than the C–Br binding energy in IndBr. Despite their lower accuracy, the data show that we can exclude any influence of dissociative photoionization below 9 eV for both radicals.

We also determined the ionization energies of the 3PPR and 1PPR radicals. As for the indenyl radical, we turned the pyrolysis on and monitored the ion and threshold electron intensity as a function of the photon energy. In Figure 7, the TPE spectrum of 3PPR is depicted, and the ion yield is shown as an inset in the figure.

We assume that the part of the spectrum between 6.9 and 7.2 eV corresponds to hot bands or sequence bands of the radical. At around 7.2 eV, the signal increases strongly. We assign this onset to the adiabatic ionization energy, $IE_{ad} = 7.20$ eV. From the rising edge of the signal, we estimate an error of about 50 meV. The TPE signal maximizes at 7.25 eV and stays roughly constant from thereon, which indicates unresolved low-energy vibrational modes, corresponding to a moderate geometry change. The ion signal of 3PPR is given as an inset in Figure 7. One also finds a signal onset at 7.2 eV for the photoionization process, using the same fitting procedure as that described above for the precursor.^{41,42} Thus, the ionization energies obtained from the total ion signal and the threshold electron signal are in agreement.

We also measured the photoionization of 1PPR, but due to the lower vapor pressure of the precursor and a lower photon flux, only a photoion yield spectrum could be obtained. In these experiments, a MgF₂ window was used to cut off higher harmonics instead of a gas filter. The spectrum is given in Figure 8. It shows that the ion signal starts at about 7.3 eV and increases over the whole energy range. A fit of the energy range from 7.25 to 8 eV gives an adiabatic ionization energy of $IE_{ad} = 7.4$ eV.^{41,42} Although the error is larger than that for the other two radicals and estimated to be 100 meV, the IE is definitely higher than that of 3PPR. The experimental IE also deviates more from the computed one than in the case of both Ind and 3PPR. In their MPI experiments, Reilly et al. placed the IE of 1PPR between 5.1 and 7.3 eV, lower than the present value. On the one hand, the error bars of the IE extracted from our 1PPR spectra are quite large, and the value presented here is thus consistent with the upper limit of this range. On the other hand,

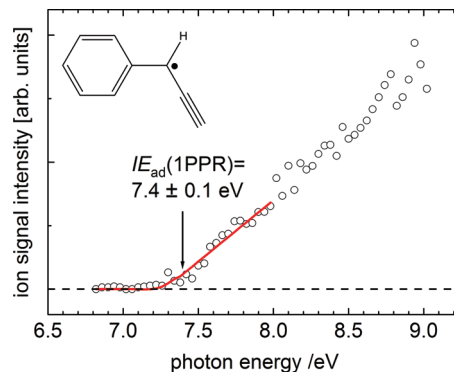


Figure 8. Photoion yield spectrum of 1PPR. The ionization energy was determined to be 7.4 ± 0.1 eV.

it is also possible that Reilly et al. ionized the radical through an intermediate Rydberg state slightly below the ionization threshold.

The IEs of both phenylpropargyl radicals have also been calculated by Reilly et al.¹³ They also used the B3LYP functional but a smaller basis set and calculated for both phenylpropargyl species an IE_{vert} of about 6.8 eV. Our calculations yielded slightly higher values that agree well with the experimental ones (see Table 1). Again, the HOMO is distributed over the complete radical in both species, a common observation for resonance-stabilized radicals. The difference in the adiabatic and vertical IEs in 3PPR is the most pronounced for any of the C₉H₇ species, in agreement with the experiment, but the computed geometry change is also small. For more information on the computations, the reader is referred to the Supporting Information. TDDFT calculations of both phenylpropargyl cations yield no excited electronic states in the experimentally studied energy range. Again, we also studied the dissociative photoionization, but no evidence of this process in 3-phenylpropargyl was observed up to a photon energy of 15 eV.

Conclusion

We investigated the photoionization of three resonance-stabilized radicals, 1-indenyl (Ind), 1-phenylpropargyl (1PPR), and 3-phenylpropargyl (3PPR), using VUV synchrotron radiation. Threshold photoelectron photoion coincidence, photoion yield, and threshold photoelectron spectroscopy were applied. All three are isomers with the same molecular formula, C₉H₇. They have been generated cleanly by jet flash pyrolysis from their bromine precursors as demonstrated by time-of-flight mass spectrometry. Our main focus was to determine the ionization energies of these radicals. We determined an adiabatic ionization energy of $IE_{ad} = 7.53$ eV for indenyl. The TPES is dominated by one strong peak, indicating a negligible geometry change. This is also confirmed by computations. Another band at around 8.1 eV is assigned to the $a^+ \ ^3B_2$ excited electronic state of the cation based on comparison with computations. It shows a vibrational progression of around 61 meV. The computed ionization energies agree well with the measured ones ($IE_{ad,calc} = 7.50$ eV; $IE_{vert,calc} = 7.54$ eV). For the phenylpropargyl radicals, the IE_{ad} could also be determined. 3PPR and 1PPR are ionized at 7.20 and 7.4 eV, respectively. The different ionization energies determined for the three isomers rule out isomerization in the pyrolysis nozzle. No excited electronic states of the cation were found in the observed energy range. Our calculations also indicate a small change in geometry during ionization. However, experimental data suggest some vibrational activity. The possibility to distinguish isomers of the same

molecular formula by photoionization was shown to be relevant for online monitoring of radicals in flames.^{6,7} The difference in the ionization energy between 3-phenylpropargyl and 1-indenyl is about 0.3 eV, and hence, a differentiation of these two isomers in flames should be possible, while a selective identification of IPPR might be more difficult. No dissociative photoionization was found for Ind and 3PPR up to 15 eV. We also investigated the photoionization and dissociative photoionization of the precursors because they dissociatively photoionize by Br-atom loss under the influence of VUV light and can also produce C₉H₇⁺ species. Appearance energies AE(C₉H₇Br, C₉H₇⁺) were determined for all three precursors. For Ind⁺ from IndBr, we obtained AE_{OK} = 10.2 eV from an analysis of the breakdown diagram and an ionization energy (IE) of 8.4 eV for the IndBr precursor from the TPES. Approximate appearance energies were also determined for the phenylpropargyl precursors. For the formation of 3PP⁺ from 3PPBr, we obtained a value of 9.8 eV, and for IPP⁺ from IPPBr, we obtained 9.3 eV. Approximate ionization energies of 8.5 (1PPBr) and 8.6 eV (3PPBr) were determined for the precursors.

Acknowledgment. This work was financially supported by the Deutsche Forschungsgemeinschaft (Fi575/7-1). Travel subsidies for P.H. were provided by the European Commission program "Transnational access to research infrastructures". We also thank Bastian Noller and Wolfgang Roth for many useful discussions and Christian Alcaraz for his contributions to preliminary experiments on C₉H₇. This work was also funded by the Swiss Federal Office of Energy (BFE Contract Number 101969/152433). This paper is dedicated to Prof. J. Weis for his contributions to Silicon chemistry on the occasion of his 65th birthday.

Supporting Information Available: Optimized geometries of the C₉H₇ radicals and cations and full ref 37. This material is available free of charge via the Internet at <http://pubs.acs.org>.

References and Notes

- (1) Kohn, D. W.; Clauber, H.; Chen, P. *Rev. Sci. Instrum.* **1992**, *63*, 4003.
- (2) Schüßler, T.; Deyerl, H.-J.; Dümmler, S.; Fischer, I.; Alcaraz, C.; Elhanine, M. *J. Chem. Phys.* **2003**, *118*, 9077.
- (3) Schüßler, T.; Roth, W.; Gerber, T.; Fischer, I.; Alcaraz, C. *Phys. Chem. Chem. Phys.* **2005**, *7*, 819.
- (4) Fischer, I.; Schüßler, T.; Deyerl, H.-J.; Elhanine, M.; Alcaraz, C. *Int. J. Mass Spectrom.* **2007**, *261*, 227.
- (5) Noller, B.; Hemberger, P.; Fischer, I.; Alcaraz, C.; Garcia, G. A.; Soldi-Lose, H. *Phys. Chem. Chem. Phys.* **2009**, *11*, 5384.

- (6) Osswald, P.; Struckmeier, U.; Kasper, T.; Kohse-Höinghaus, K.; Wang, J.; Cool, T. A.; Hansen, N.; Westmoreland, P. R. *J. Phys. Chem. A* **2007**, *111*, 4093.
- (7) Taatjes, C. A.; Klippenstein, S. J.; Hanson, N.; Miller, J. A.; Cool, T. A.; Wang, J.; Law, M. E.; Westmoreland, P. R. *Phys. Chem. Chem. Phys.* **2005**, *7*, 806.
- (8) Li, Y.; Zhang, L.; Tian, Z.; Yuan, T.; Wang, J.; Yang, B.; Qi, F. *Energy Fuels* **2009**, *23*, 1473.
- (9) Taatjes, C. A.; Hansen, N.; Osborn, D. L.; Kohse-Höinghaus, K.; Cool, T. A.; Westmoreland, P. R. *Phys. Chem. Chem. Phys.* **2008**, *10*, 20.
- (10) Pottier, R. F.; Lossing, F. P. *J. Am. Chem. Soc.* **1963**, *85*, 269.
- (11) Izumida, T.; Inoue, K.; Noda, S.; Yoshida, H. *Bull. Chem. Soc. Jpn.* **1981**, *54*, 2517.
- (12) Andrews, L.; Kelsall, B. J. *J. Phys. Chem.* **1987**, *91*, 1435.
- (13) Reilly, N. J.; Kokkin, D. L.; Nakajima, M.; Nauta, K.; Kable, S. H.; Schmidt, T. W. *J. Am. Chem. Soc.* **2008**, *130*, 3137.
- (14) Reilly, N. J.; Nakajima, M.; Gibson, B. A.; Schmidt, T. W.; Kable, S. H. *J. Chem. Phys.* **2009**, *130*, 144313.
- (15) Alkemade, U.; Homann, K. H. *Z. Phys. Chem.* **1989**, *161*, 19.
- (16) Miller, J. A.; Melius, C. F. *Combust. Flame* **1992**, *91*, 21.
- (17) Morter, C. L.; Farhat, S. K.; Adamson, J. D.; Glass, G. P.; Curl, R. F. *J. Phys. Chem.* **1994**, *98*, 7029.
- (18) Stein, S. E.; Walker, J. A.; Suryan, M. M.; Fahr, A. *Proc. Combust. Inst.* **1990**, *23*, 85.
- (19) Bodi, A.; Johnson, M.; Gerber, T.; Gengeliczki, Z.; Sztáray, B.; Baer, T. *Rev. Sci. Instrum.* **2009**, *80*, 034101.
- (20) Johnson, M.; Bodi, A.; Schulz, L.; Gerber, T. *Nucl. Instrum. Methods Phys. Res., Sect. A* **2009**, DOI:10.1016/j.nima.2009.08.069.
- (21) Baer, T. *Int. J. Mass Spectrom.* **2000**, *200*, 443.
- (22) Baer, T.; Guyon, P.-M. *High Resolution Laser Photoionisation and Photoelectron Studies*; Wiley: New York, 1995.
- (23) Whitaker, B. J. *Imaging in Molecular Dynamics*; Cambridge University Press: Cambridge, U.K., 2003.
- (24) Sztáray, B.; Baer, T. *Rev. Sci. Instrum.* **2003**, *74*, 3763.
- (25) Garcia, G. A.; Soldi-Lose, H.; Nahon, L. *Rev. Sci. Instrum.* **2009**, *80*, 023102.
- (26) Buu-Hoi, N. P. *Liebigs Ann.* **1943**, *556*, 1.
- (27) Lian, J.-J.; Chen, P.-C.; Lin, Y.-P.; Ting, H.-C.; Liu, R.-S. *J. Am. Chem. Soc.* **2006**, *128*, 11372.
- (28) Smith, L. I.; Swenson, J. S. *J. Am. Chem. Soc.* **1957**, *79*, 2962.
- (29) Baer, T.; Sztáray, B.; Kercher, J. P.; Lago, A. F.; Bodi, A.; Skull, C.; Palathinkal, D. *Phys. Chem. Chem. Phys.* **2005**, *7*, 1507.
- (30) Jarvis, G. K.; Weitzel, K. M.; Marlow, M.; Baer, T.; Song, Y.; Ng, C. Y. *Phys. Chem. Chem. Phys.* **1999**, *1*, 5259.
- (31) Weitzel, K. M.; Marlow, M. *J. Chem. Phys.* **1999**, *111*, 8267.
- (32) Beyer, T.; Swinehart, D. F. *Commun. ACM* **1973**, *16*, 379.
- (33) Levenberg, K. *Quart. Appl. Math.* **1944**, *2*, 164.
- (34) Marquardt, D. *J. Appl. Math.* **1963**, *11*, 431.
- (35) Dewar, M. J. S.; Haselbach, E.; Worley, S. D. *Proc. R. Soc. London* **1970**, *A315*, 431.
- (36) Lee, C.; Yang, W.; Parr, R. G. *Phys. Rev. B* **1988**, *37*, 785.
- (37) Frisch, M. J.; et al. *Gaussian 03*, revision D.01; Gaussian Inc.: Wallingford CT, 2004.
- (38) Csaszar, P.; Pulay, P. *J. Mol. Struct.* **1984**, *114*, 31.
- (39) Perdew, J. D. *Phys. Rev. B* **1986**, *33*, 8822.
- (40) Becke, A. D. *J. Chem. Phys.* **1993**, *98*, 5648.
- (41) Asher, R. L.; Appellmann, E. H.; Ruscic, B. *J. Chem. Phys.* **1996**, *105*, 9781.
- (42) Guyon, P. M.; Berkowitz, J. *J. Chem. Phys.* **1971**, *54*, 1814.